

Fractal Analysis of Fracture Systems

Topical Report
September 3, 1996

RECEIVED
AUG 14 1997
OSTI

Work Performed Under Contract No.: DE-FG21-92MC32158

For
U.S. Department of Energy
Office of Fossil Energy
Federal Energy Technology Center
Morgantown Site
P.O. Box 880
Morgantown, West Virginia 26507-0880

DISTRIBUTION OF THIS DOCUMENT IS UNLIMITED

[Handwritten signature]

By
West Virginia University
Department of Geology and Geography
425 White Hall
P. O. Box 6300
Morgantown, West Virginia 26506-6300

MASTER

19980313 063

DTIC QUALITY INSPECTED 4

Disclaimer

This report was prepared as an account of work sponsored by an agency of the United States Government. Neither the United States Government nor any agency thereof, nor any of their employees, makes any warranty, express or implied, or assumes any legal liability or responsibility for the accuracy, completeness, or usefulness of any information, apparatus, product, or process disclosed, or represents that its use would not infringe privately owned rights. Reference herein to any specific commercial product, process, or service by trade name, trademark, manufacturer, or otherwise does not necessarily constitute or imply its endorsement, recommendation, or favoring by the United States Government or any agency thereof. The views and opinions of authors expressed herein do not necessarily state or reflect those of the United States Government or any agency thereof.

Fractal Analysis of Fracture Systems

*Prepared by Tom Wilson -
Dept. of Geology and Geography
West Virginia University*

Introduction

A fractal analysis of outcrop fracture patterns was undertaken in the Valley and Ridge study area (Figure 1). Use of pavement style investigations such as those conducted by Barton and Hsieh (1989) was not a feasible form of analysis in either Appalachian study areas. Large exposures of bedding plane surfaces are limited, particularly at the Plateau site; hence, fracture studies were concentrated in the Middle and Elkhorn Mountain areas of the Valley and Ridge. The area is complexly deformed (Figure 1), which presented difficulty in the design of a controlled experiment. While bedding plane exposures were found, it was not possible to find comparable exposures of the same lithologic unit in the different structural areas represented at the site. In such instances, therefore, lithologic factors could not be separated from structural factors in the interpretation of variations in fractal dimension. Comparisons of fractal behavior in a common lithologic interval were possible to some extent using one-dimensional analysis of bed-normal fracture plane intersections. However, even in this case, the distribution of exposure was the limiting factor.

Within the context of these restrictions, the analysis of the data presented below give rise to important considerations in the use of fractals characterization of fracture networks. For example, some of the largest differences in fractal dimension were observed in the same outcrop in units separated by a vertical distance of less than a meter. Large differences also appear between the fractal dimensions of systematic and non systematic fractures observed at a single outcrop. Fluid transport within a reservoir is probably controlled moreso by the larger more pervasive regional scale joint sets (Lorenz et al. 1996). Hence, accurate fractal characterization of reservoir fracture networks must separate the influence of systematic and nonsystematic joint sets. Based on the results of Walsh and Wattersen (1993) the viability of

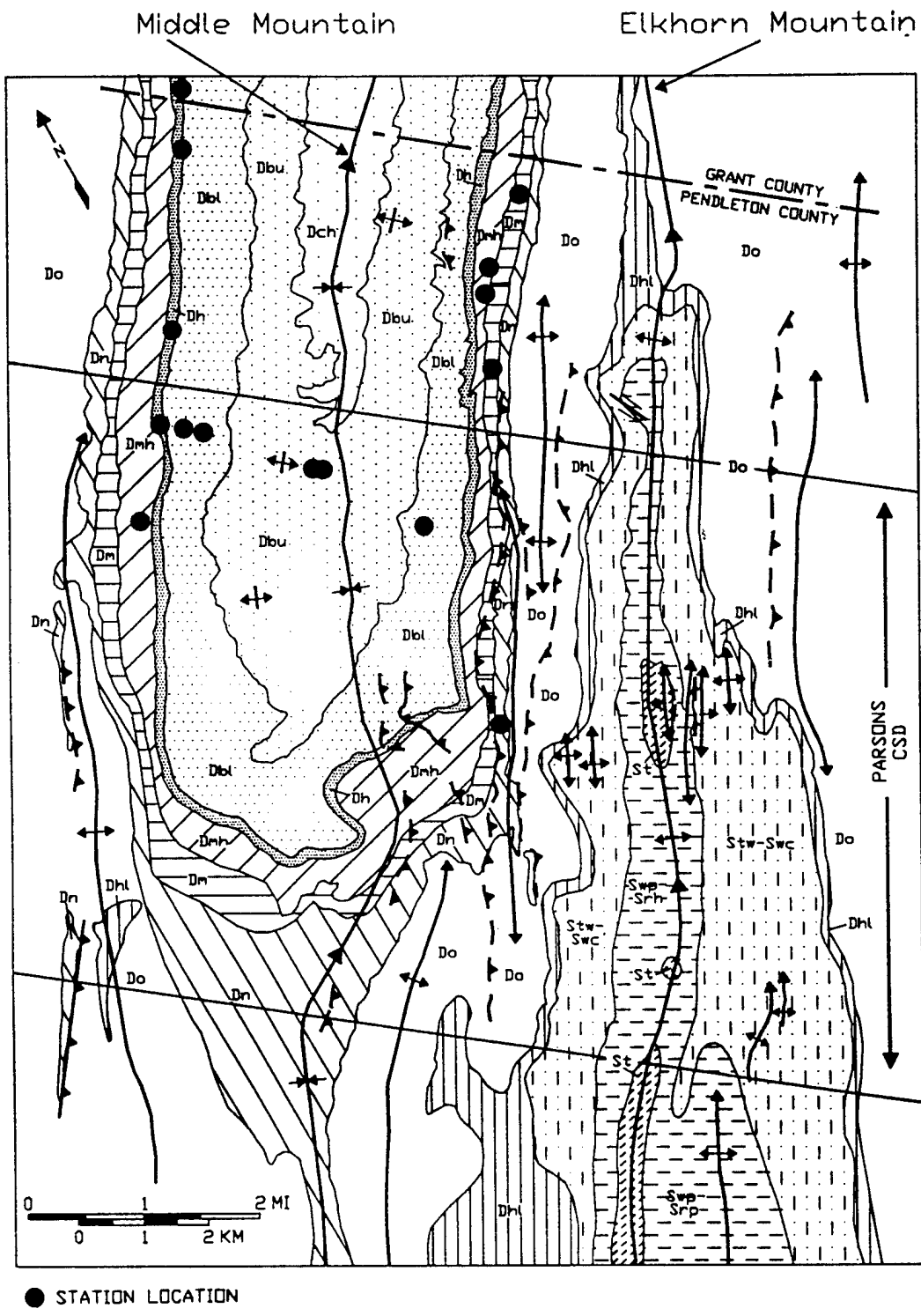


Figure 1: Fracture observations were made at several locations (large black dots) within the Valley and Ridge study area.

the fractal model of fracture networks must also be reevaluated. The results presented here are even more condemning of the blind use of a fractal model of fracture networks.

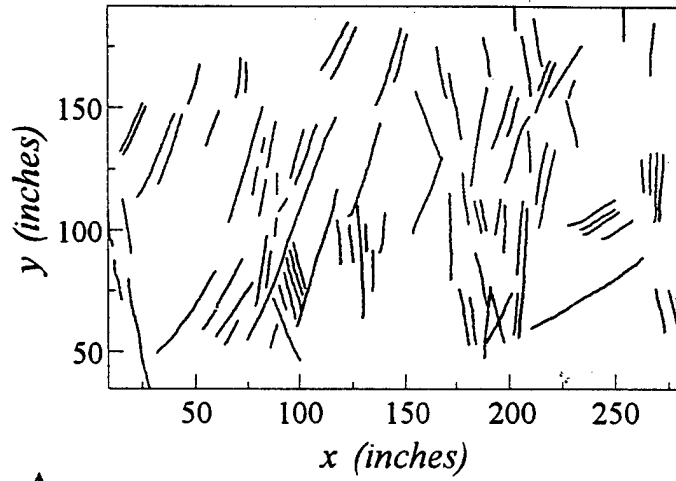
Methods

Fracture patterns were photographed at several locations within the area (Figure 1). Most of the sites are located in the Devonian shales which are confined to the northwest and southeast limbs of Middle Mountain syncline. The Devonian shales exposed in this area are the Valley and Ridge equivalent of intervals buried beneath the Plateau which form significant fractured reservoirs of natural gas. The Devonian shales are easily eroded and form the major valleys through the area. Road cuts along the valley provided numerous exposures which were large enough to undertake fractal analysis of fracture patterns. Exposures elsewhere in the study area did not provide sufficient numbers of fracture plane intersections to evaluate. This observation in itself is foretelling of the non-fractal nature of fracture systems. Observations were also made across the axis of the Middle Mountain syncline where road cuts provided several good exposures (Figure 1).

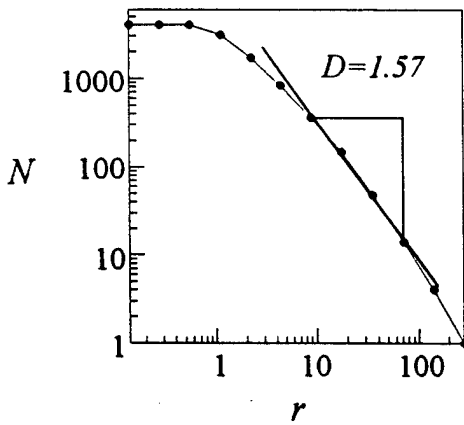
In Chapters 2 and 4 (final report, in preparation) we note that box counting of fault and drainage patterns generally do not yield a fractal regime. The slope of the boxplot ($\log N$ vs. $\log r$ plot) is often 2 over the first 4 to 5 base 2 orders. Beyond that, further reductions of box size yield non-linear $\log N - \log r$ response. In this *topical report*, we see that this non-linear response is also common in box counting data from fracture networks. In such instances, the results of box counting provide what is probably best referred to as a quasi-fractal measure of pattern complexity. Before evaluating and comparing fracture patterns, we present boxplots which are typical of fracture data collected in this study. Basic features of the $\log N / \log r$ plot are illustrated, and the approach used to evaluate and compare the $\log N / \log r$ data is defined.

As an example, fracture patterns observed on the northwest limb of the Middle Mountain syncline (Figure 2A) yield the $\log N - \log r$ plot shown in Figure 2B. Variations in the number of occupied boxes with changes in box size rise almost linearly but then begin to show noticeable flattening for smaller and smaller box sizes. Similar behavior is noted by Walsh and Wattersen (1993) in their reevaluation of Pavement 1000 from Barton and Hsieh (1989) in the Yucca Mountain area and for active fault patterns observed in Japan (Wilson and Dominic, in review).

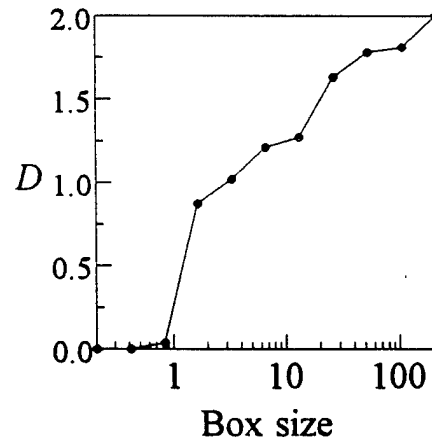
Some of the features in Figure 2B are anticipated. For example, the initial box is always occupied since it covers the entire area; and unless the distribution of fractures is very sparse, the next subdivision will yield 4 occupied. It is the rate at which smaller size boxes turn up empty that defines the fractal characteristics of the pattern. If boxes at successively smaller scales



A.



B.



C.

Figure 2: Fracture patterns traced from a photograph (A) yielded the $\log N$ vs. $\log r$ plot shown in (B). The point-to-point variation in fractal dimension observed in the $\log N$ vs. $\log r$ plot are shown in C.

are all occupied, the slope of the logN-logr plot is 2 (i.e. $D = 2$). When all boxes are occupied, the number of occupied boxes increases as the square of the number of boxes along the map edge. Since the number of boxes covering the map edge increases as $(1/r)^2$, the log-log slope or fractal dimension is 2.

The point-to-point slope changes in the log N vs. log r plot (Figure 2B) are shown in Figure 2C. In this case, all the boxes are occupied in the first two coverings (1 box and 4 boxes). Calculation of the slope between these two points is 2. The values plotted in Figure 2C are plotted at the midpoint between consecutive values of r . For box sizes less than 100 inches in size along the x-axis, unoccupied boxes are encountered. Point-to-point values of D fall below 2 and drop down to 0 for box sizes of about 1 inch and less.

The region of Figure 2C where D drops to 0 results from the discrete nature of the fracture trace data. Fracture traces are digitized at a certain sampling interval, and thus there are a finite number of samples in the data set. The data shown in Figure 2A were sampled at approximately 1 inch intervals. When the box size is less than the sampling interval, the number of occupied boxes will equal the total number of samples in the data set. Further decreases of box size yield no increase in the number of occupied boxes and the slope of the curve in this region becomes 0 (Figure 2B and 2C).

The $D=0$ region and the transition to it are always encountered in digital data. If our data were comprised of continuous line segments, rather than samples, a reduction in box size by 1/2 would double the number of occupied boxes, and we would eventually end up in a non-fractal region with $D = 1$. The scale at which the transition to 0 (or 1) occurs may represent a resolution limit below which finer details are not representable. This transition may also indicate that at finer scale, additional detail is, in actuality, not present. Fracture patterns might have fractal dimension less than 1 if they consist of sets of disconnected segments analogous to that of the Cantor set, for example.

Regions of the log N vs. log r plot where $D = 2$, and D approaches 0 are associated with artifacts of the initial box covering and digital form of the data and provide no useful information about the pattern. Our primary interest is to find a truly fractal region of constant slope in the log N vs. log r plot. If it existed, it might appear as a flattened region in Figure 2C.

A clearly defined fractal region was not observed in the fracture patterns measured for this study. There is nothing unusual about the patterns, which suggests that fracture patterns may, in general, be non-fractal, or only close to fractal over a limited scale range. Walsh and Wattersen (1993) make similar observations but stop short of declaring fracture patterns to be non-fractal. Instead, they suggest that fractal analysis should be confined to a scale range that lies between the largest and smallest fracture spacing represented in the data set. In the following study the analysis is carried out over a consistent scale range referenced to the photographs from which the patterns were

digitized. Since the fracture patterns were digitized from photographs of outcrops, the actual scale range varies, but corresponds approximately to the 1-to-0.1 inch scale range of the photograph itself.

A second example presented in Figure 3 is taken from the southeast limb of the Middle Mountain syncline. In all cases, D is computed for the third through sixth data points from lower right of the $\log N$ vs. $\log r$ plot (Figure 3B). This range of points corresponds to an outcrop scale range of approximately 8-to-1 inches and to the 0.1-to-1 inch scale range of the photograph. To save computing time the computations were not carried out for very small boxes, so that the flattened response observed in Figure 2B (upper left of plot) does not appear. Slight curvature is observed in the $\log N$ vs $\log r$ plot through the 4-point region (e.g. Figure 2B) for which the slope was calculated, however, the correlation coefficient for the slope of the regression line over this range of scales on the photograph is always greater than 0.99.

Fracture Analysis

The interpretation and significance of box counting analysis is a recurrent theme in the chapters of the final report (in preparation). If fracture networks are truly fractal, then the patterns observed at different scales should have similar fractal dimension. As noted by Walsh and Wattersen (1993), there is continuous variation in the slope of the $\log N$ vs. $\log r$ plot for examples of pavement taken from Barton and Hsieh (1989). This point has just been illustrated above using data from this study, and the suggestion to compute the fractal dimension over a range of scales accurately represented in the data (Walsh and Wattersen 1993) is adhered to in the following analysis. However, we further question the viability of the fractal model by analyzing both large and small scale photographs of the same outcrop.

Two examples are shown in Figure 5. Figures 5A and 5B represent small and large scale photographs of the same outcrop. The fracture patterns observed in the small rectangular region highlighted in Figure 5A are shown in Figure 5B. Additional detail appears in the finer scale photograph, but the pattern is less densely fractured. The change of appearance is represented by a decrease in fractal dimension from 1.74 (Figure 5A) to 1.47 (Figure 5B).

$\log N$ vs. $\log r$ plots for both patterns are shown in Figure 6. Individual point-to-point slopes are shown over the range used to compute D . The slope between points covering the range 18.25-9.2 inches in the small scale pattern (Figure 5A and 6A) is approximately 1.47 while over a similar range (14.25-7.125 inches) in the large scale photograph (Figure 5B and 6B) the slope is 1.82. The larger scale or finer detail scrutiny of the outcrop reveals an increasingly complex pattern, but over the range of scales represented in the finer scale photograph, D is smaller. Additional fractures appear at finer scales, but overall their relative density decreases.

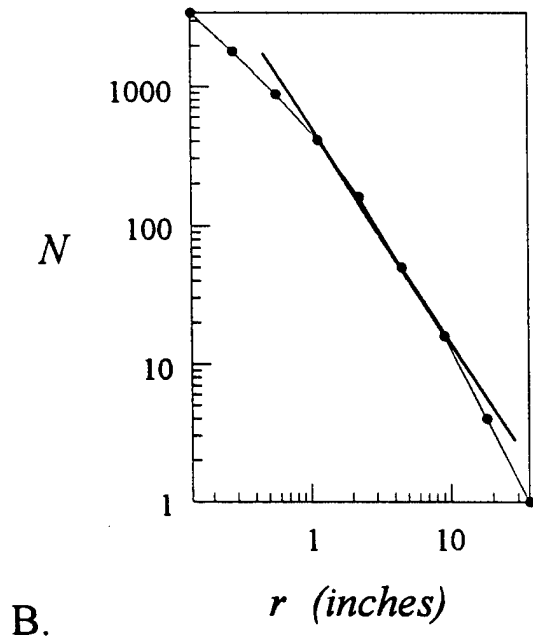
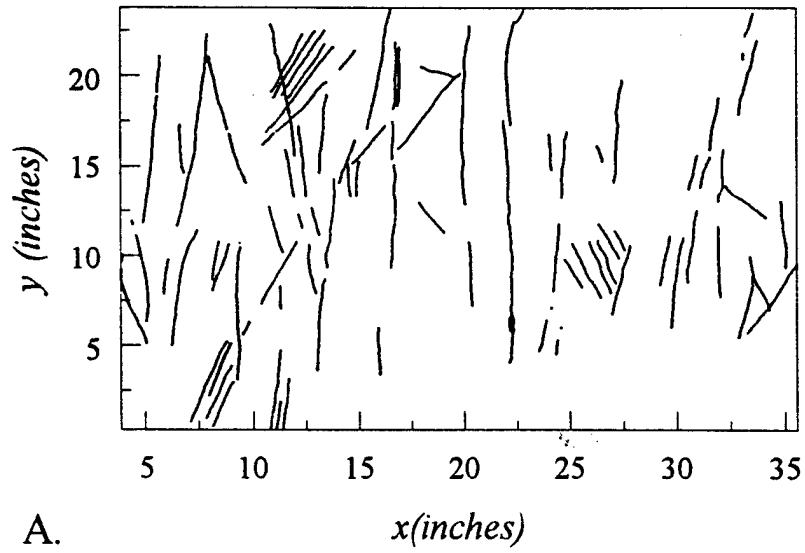


Figure 3: Another example of the typical $\log N$ vs. $\log r$ response observed in the fracture patterns sketched at another location (A) is shown in (B).

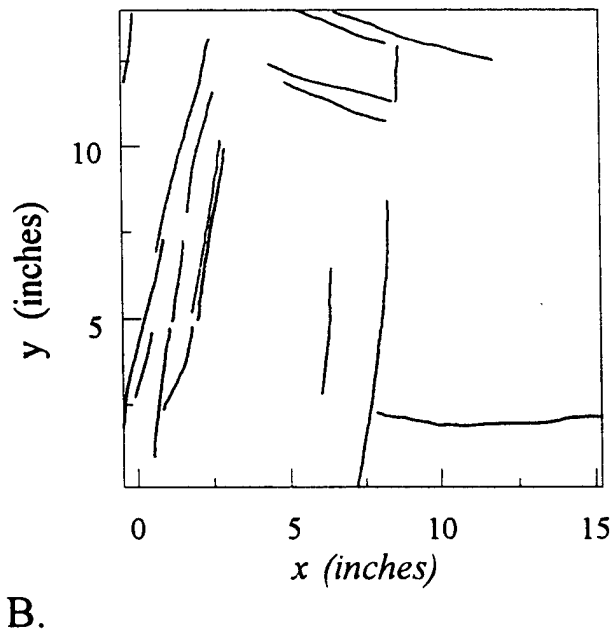
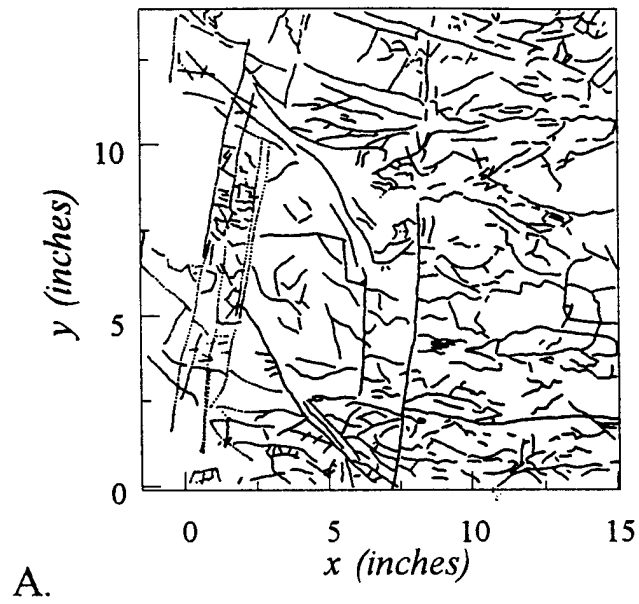
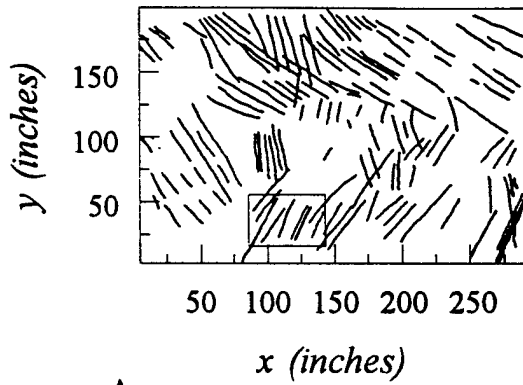
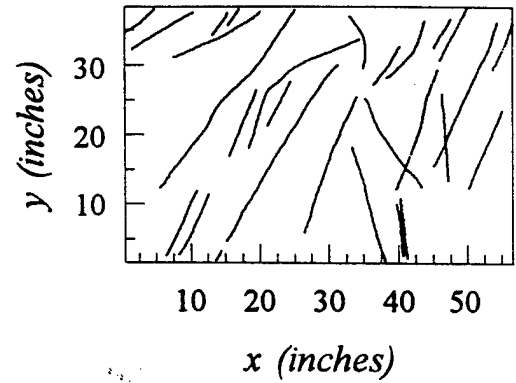


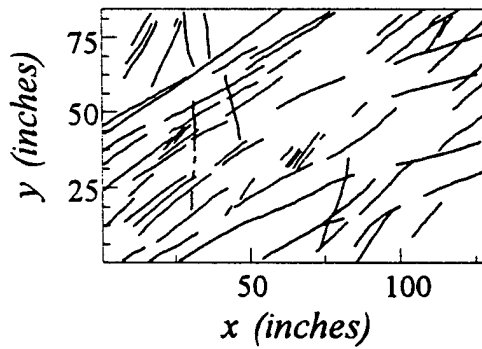
Figure 4: Fracture patterns in (A) portray both systematic and non-systematic fracture sets. The systematic fracture sets present at this site are portrayed in (B).



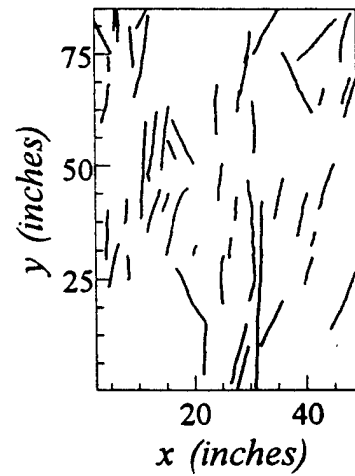
A.



B.

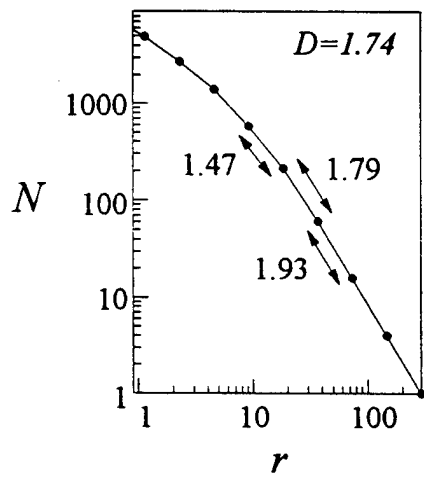


C.

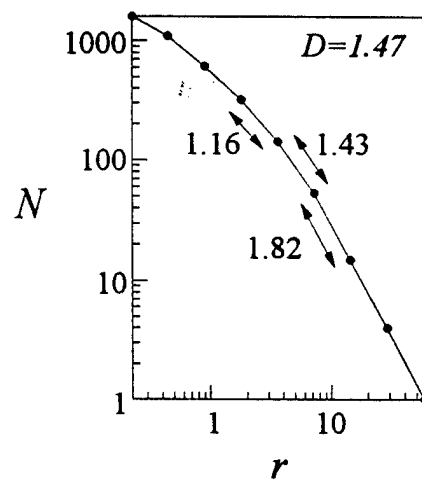


D.

Figure 5: The influence of scale is illustrated in the sketches presented here. The small rectangular area marked located in pattern (A) represents the location of the close-up pattern shown in (B). Pattern (C) is compared to a nearby close-up (D).



A.



B.

Figure 6: The $\log N$ vs. $\log r$ plots for patterns A and B of Figure 5 are presented here in (A) and (B) respectively.

Another example is presented in Figures 5C and 5D. In this case the fractal dimension decreases from 1.67 to 1.37 from the coarse to finer scale. The camera angle displayed in Figure 5D is rotated into alignment with the dominant left-dipping fracture trend present at the site. The field of view (Figure 5D) does not fall within the view covered in Figure 5C but was taken within the same outcrop.

The result suggests that fracture patterns are not fractal, or at best, that their fractal characteristics are non-stationary (a contradiction in terms). Within the context of these results, it is necessary to photograph and compare a similar scale range in order to make valid comparisons of pattern complexity using fractal measures of pattern complexity.

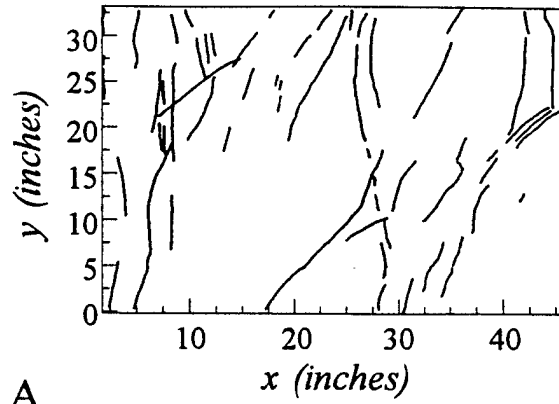
2D Fractal Characterization

Characterization of fracture patterns observed at several sites in the Middle Mountain and Elkhorn Mountain area (Figure 1) are evaluated in the following discussions. Box counting data are used to determine the fractal dimension of individual patterns, although the validity of the fractal model is considered questionable as noted above.

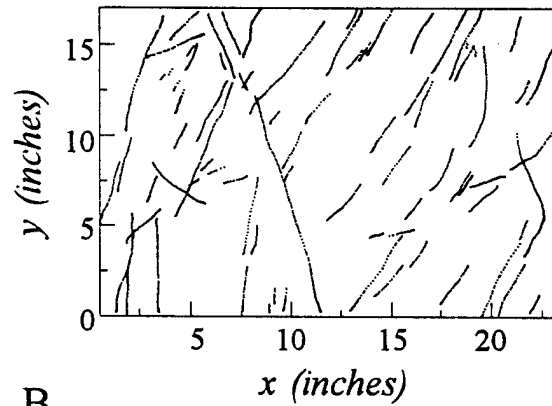
Fracture patterns sketched from photographs of outcrops along the southeast limb of the Middle Mountain syncline are shown in Figure 7. Fractal dimensions of patterns A through C are 1.49, 1.49, and 1.57 respectively. Patterns A and B lie in the area north of the Parsons CSD, while pattern C was measured in an outcrop located within the CSD. At first glance, there appears to be a slight increase in the fractal dimension of the fracture patterns observed in the CSD. However, note that the scale range covered in pattern B extends over little more than half the range covered in A and C. Based on the observations presented in the preceding section, it is likely that if an equivalent area were exposed in the vicinity of B (Figure 7B) the fractal dimension would increase.

Recomputation of the fractal dimension for subdivision of these patterns into 15 by 15 inch regions confirms this suspicion. Average fractal dimensions of 1.1, 1.41 and 1.43 were obtained for patterns A, B and C respectively. Individually they are less than values calculated for the entire pattern because in all cases D was computed over a smaller, but common, area. This approach also appears to more accurately represent the visual differences apparent in these patterns.

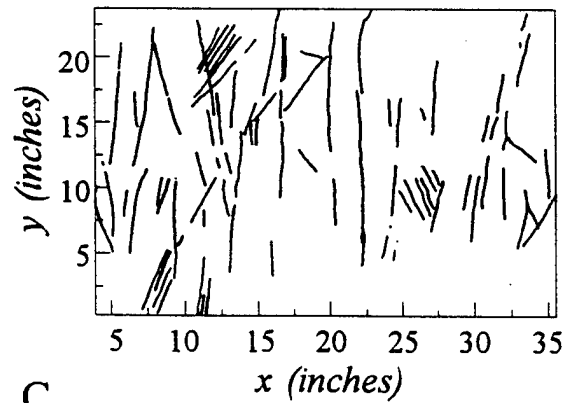
Sketches of fracture patterns observed on the northwest limb of Middle Mountain syncline are shown in Figure 8. These patterns also show increasing levels of complexity that are almost certainly due to the increasing field of view. D increases from 1.37, 1.45, and 1.57 for patterns A through C respectively (Figure 8). Computation of fractal dimensions for 45 by 45 inch subdivisions of these patterns yields average fractal dimensions of 1.28, 1.23,



A.



B.



C.

Figure 7: Fracture patterns observed along the southeast limb of the Middle Mountain syncline are presented from two areas northeast of the Parsons CSD (A and B) and from within the CSD (C).

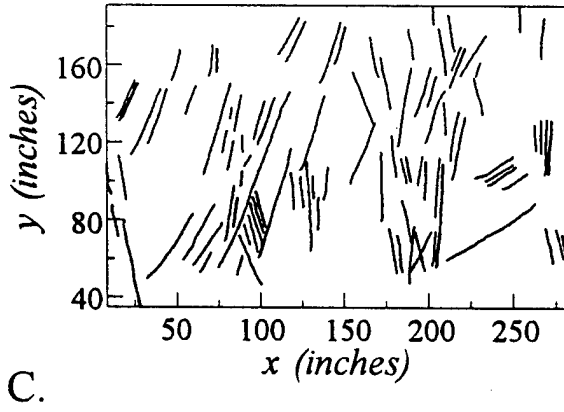
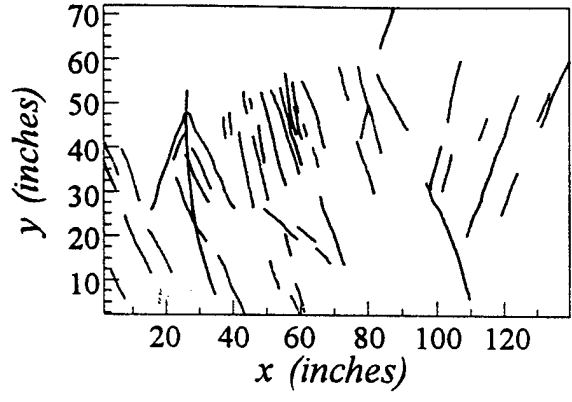
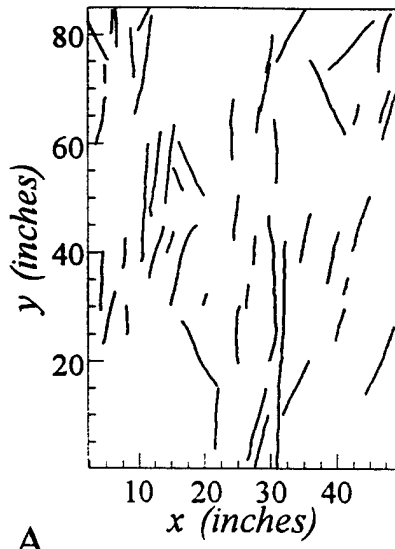


Figure 8: Fracture patterns observed along the northwest limb of the Middle Mountain syncline are presented for two areas northeast of the Parsons CSD (A and B) and from one within the CSD (C).

and 1.1 for patterns A through C respectively, reversing the results obtained from the entire field of view. There are also problems with subdividing the smaller scale photographs into 40 x 40 inch subdivisions. For example, sketch C covers a 282 x 191 inch area so that features at the 40 x 40 inch scale are underrepresented or not equivalent to those obtained from photographs taken closer to the outcrop.

In general, the applicability of a fractal model is brought into question by the field studies undertaken in this phase of the research. Disappointingly, we must conclude that results obtained from the analysis of more than 30 exposures reveal no differences of structural significance. This, however, does not minimize the importance of these results. The acceptance and implementation of fractal models of fracturing into reservoir simulations should not be pursued without confirmation of the fractal nature of these fracture systems. Having established this as a significant research question, we feel that future work needs to be directed toward studies designed specifically to evaluate the viability of a fractal model of fractal networks. Structural differences may exist, however, but future assessment of fracture patterns, if it should be undertaken, will photographing patterns at common scale.

1D Analysis

Evaluations of fracture patterns were also undertaken using one-dimensional fracture intersection data. These data sets were compiled by marking off fracture intersection points measured along vertical slices through a rock layer. Siltstones within the Braillier Formation form a prominent and traceable unit in parts of the Valley and Ridge study area, particularly along the northwest limb of the Middle Mountain syncline, and, in places, along its axis. In most cases, these exposures present vertical sections through the formation. The silts display prominent fracture sets, which may or may not extend vertically into surrounding rock intervals. Analysis of the silts provided the possibility of conducting a controlled experiment, since comparisons of the fractal characteristics of fracture systems could be conducted in several areas while lithology and stratigraphic level could be held roughly constant.

A modified version of the box-counting program was used to compute the fractal dimension of fracture intersections encountered along the silt layers. The analysis was restricted to 4-6inch silts. The data sets collected here are equivalent to those which might be encountered in a horizontal well. This experiment is of particular interest since it also allows us to evaluate the accuracy of fractal characterization made from the limited exposure provided by the borehole. The data collected for this experiment were obtained by direct measurement of fracture distance from a common reference point along the layer. Vertical differences observed in a single outcrop were noted in some instances.

An example of the horizontal fracture intersection patterns observed in this study are shown in Figure 9A. The locations of fractures cutting through this siltstone were measured in the field. A 4.28 foot length of the siltstone is shown in the photograph. Fracture intersections (Figure 9B) were measured off along approximately 25 feet of continuous exposure.

The anticipated range of fractal dimension obtained from such data extends from 0 to 1. Features of the $\log N$ vs. $\log r$ plot (Figure 9C) mentioned previously in the analysis of two-dimensional patterns are also encountered in the one-dimensional results. The $\log N$ vs. $\log r$ plot flattens out as r approaches the minimum fracture spacing encountered in the set. Another example (Figure 10) reveals similar $\log N$ vs $\log r$ behavior. The response is typical of the siltstone fracture patterns encountered in this area.

The distribution of siltstones through the area is not uniform. They are frequently observed on the northwest limb of the Middle Mountain syncline, but rarely observed on the southeast limb. A transect through the syncline (Figure 1) suggests that the reduced number of silts encountered on the southeast limb of the syncline is the result of a facies change. The presence of silts also appears to diminish northeast-to-southwest across the CSD. The distribution of silts may simply be the result of facies changes in the area; however, the southeast limb of the syncline is more intensely deformed (Wilson 1986) and the absence of siltstone exposure in the lower Brailier may also be due in part to higher erosion rates in this more intensely deformed area.

The distribution of silts through the area made it possible to compare the fractal characteristics of fracture distribution within and out of the CSD along the northwest limb of the Middle Mountain syncline, and also along a transect across the syncline along the northern border of the CSD. The average fractal dimension of the fracture patterns within (0.85 ± 0.05) and out (0.82 ± 0.07) of the CSD are not statistically different. The fractal dimension of fracture patterns observed within the discontinuity on the axis of the syncline ($D=0.88$) and its southeast limb ($D = 0.83$) are not significantly different from each other; nor do they differ from the average fractal dimension of fracture patterns measured on the northwest limb of the syncline ($D = 0.84$) at locations also within the discontinuity. Interestingly enough, the greatest difference in fractal dimension (D s of 0.75 and 0.87) was observed between two silts, less than a meter apart within the same outcrop. Differences in the fracture patterns measured in these siltstones (Figure 11) do not appear related to local structures such as faults or folds. The intervals from which these measurements were taken is flat lying and undeformed.

1D and 2D Interrelationships

One-dimensional analysis yielded fractal dimensions that ranged from 0.75 to 0.92. On the average the fractal dimension of the fracture plane/bed-

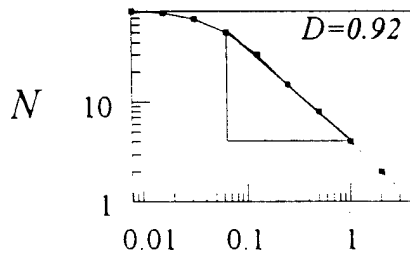


A.



B.

x (ft)



C.

Figure 9: A photograph of a siltstone typical of those found throughout the Braillier Formation is shown in (A). The distribution of fractures along this exposure are shown in (B). The log N vs. log r plot is presented for this pattern in (C).

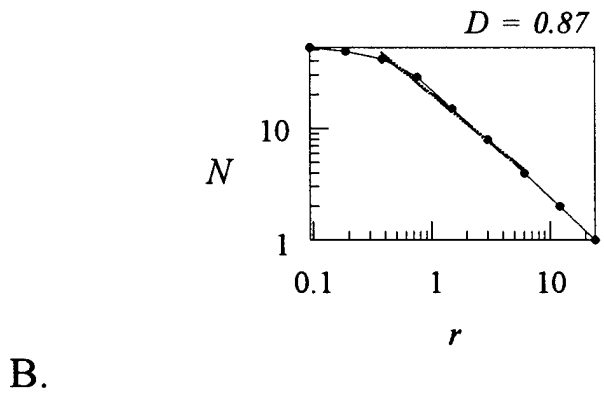
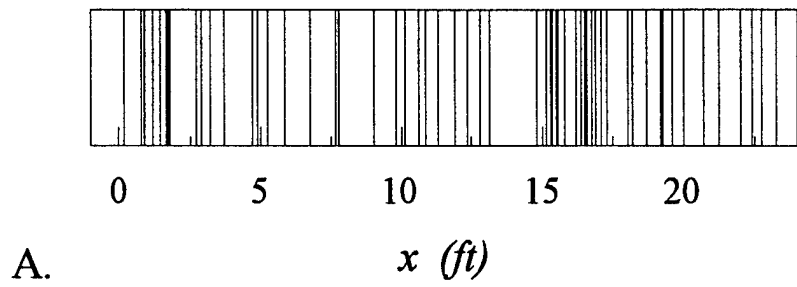


Figure 10: Patterns observed at another site (A) are presented (A) along with the corresponding $\log N$ vs. $\log r$ plot (B).

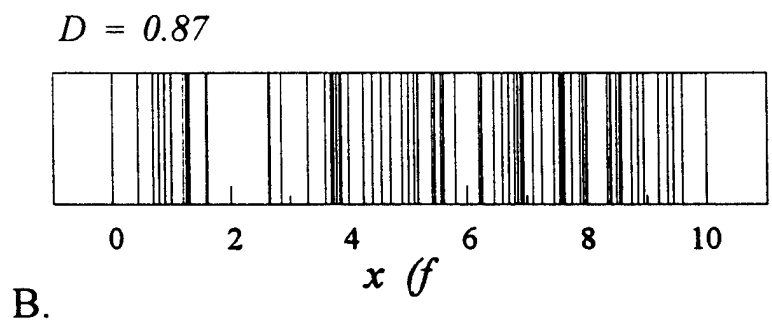
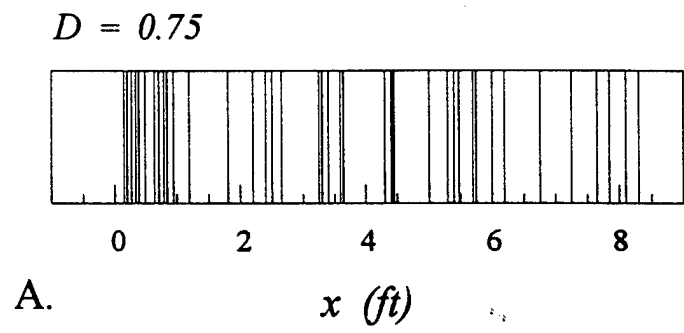


Figure 11: Fracture patterns measured at the same outcrop in siltstones of similar thickness separated by about 1m are presented in A and B. Their fractal dimensions represent the largest differences encountered in these investigations.

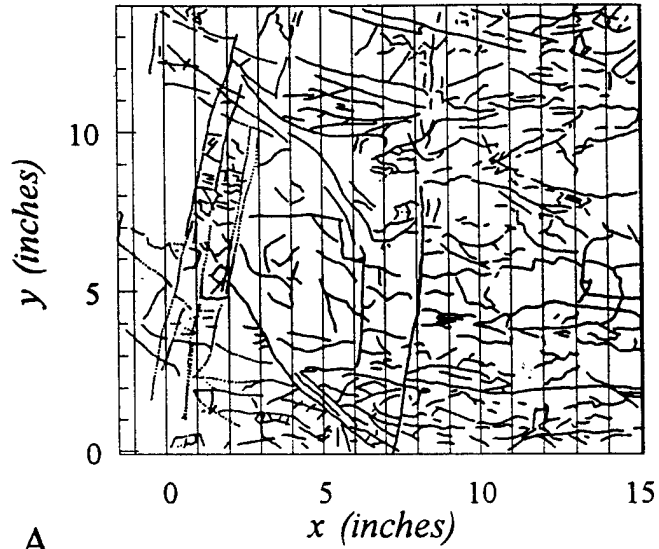
normal intersection patterns is 0.84 ± 0.05 . Turcotte (1992) argues that the fractal dimension of planar cross sections through a fractured volume of rock (D_2) are simply related to the fractal dimension of the rock volume (D_3) by the relationship $D_3 = D_2 + 1$. It is hard to carry this analogy from two to one dimensional representations. Inspection of Turcotte's fragmentation model suggests that results extending from $D = 1$ to approximately 0 will occur depending on the orientation of a line across the surface of his model. Rather than deal with these possibilities from a theoretical point of view, we examine the relation empirically by computing the fractal dimension of fracture intersections with several linear transects across one of the two-dimensional patterns observed in the field. The results of a theoretical analysis also seem inapplicable in these studies since the strict assumption that these fracture patterns are fractal has not been verified by observation. We undertake this analysis on the pattern presented in Figure 4. Fracture intersections were measured along 17 transects through the pattern (Figure 12). While the fracture patterns in this sketch do not cover linear dimensions comparable to those measured in the siltstones, the comparison will be internally consistent and provide a general representation of relative differences to be expected between one- and two-dimensional analysis. We also make the assumption that the preponderance of fractures measured in the siltstone layers are actually non-systematic fractures. This assumption is supported by the observation that the majority of fracture intersections observed in the siltstone are confined to the siltstone layer.

The fractal dimension of the two-dimensional pattern is 1.91. The fractal dimensions computed for each of the transects through the pattern ranged from 0 to 0.72. The average fractal dimension is 0.55 ± 0.18 . Based on this limited test, it seems imprudent to suggest that the fractal dimensions of one-dimensional fracture distributions can be guessed from those of the corresponding two-dimensional patterns.

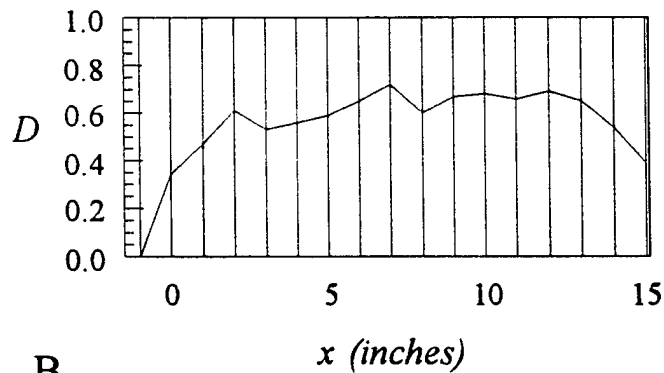
Conclusions

The results of the foregoing studies suggest that fracture distributions are not fractal. Major findings of this analysis include the following.

- Patterns formed by fracture systems are considerably more complex than currently addressed in the literature. The observations presented here suggest that pattern complexity decreases with the area of investigation. Effort needs to be expended to evaluate the validity of fractal representations fracture systems. Perhaps fractal models are justifiable in some areas. However, observations such as those presented above, made at different scales, need to be presented to verify such assertions.



A.



B.

Figure 12: Results from an evaluation of 1D estimates of fractal dimension extracted from a 2D pattern. The fracture patterns shown in (A) were sampled at 1 inch intervals along the x axis. Variations in the fractal dimensions of each 1D set are plotted in (B).

- If, in other areas, a fractal model is valid, then it will be necessary to assess the relative importance of systematic vs. non-systematic fracture networks in applications such as those associated with reservoir modeling of fluid flow. Models based on the results of fracture studies incorporating both systematic and non-systematic fractures are likely to yield significant differences from those incorporating only the systematic fracture systems.
- Although the fractal model is invalid in the Valley and Ridge area, future use of fractal statistics could be employed to quantify pattern complexity at different scales. Measurements over several ranges of scale would be required. The fractal dimension of fracture systems measured over large areas is invariably greater than that measured over smaller areas. Perhaps non-linear variations in pattern complexity can be established, which will allow extrapolation of pattern complexity outside the observable scale range, and even numerical modeling.
- In the same vein, the failure of the fractal model requires that future implementation of fractal statistics in the evaluation and comparison of fracture data from this area must be standardized. Log N vs. log r slopes must be computed over a constant scale range to obtain comparable numerical estimates.
- Exceptions to the fractal model arise primarily within the context of box counting data. The results obtained here do not affect results obtained through use of the roughness-length or compass methods of fractal dimension estimation discussed in our earlier studies.
- If the results this study area considered within the context of potential wellbore evaluations of fracture networks, it is unlikely that computed fractal dimensions obtained from the wellbore will accurately represent the fractal dimension of the systematic fracture network in the surrounding reservoir. This discrepancy is likely to arise regardless of the applicability of the fractal model, unless systematic and non-systematic fracture sets are differentiated.
- The results obtained from this analysis bring into question the general applicability of reservoir simulations employing fractal models of fracture distribution.

References

- Barton, C. C., and Hsieh, P. A., 1989, Physical and hydrologic- flow properties of fractures; 28th International Geological Congress Field Trip Guidebook T385, *American Geophysical Union*, Washington, D. C., p. 36.
- Lorenz, J. C., Warpinski, N. R., and Teufel, L. W., 1996, Natural fracture characteristics and effects: *The Leading Edge*, vol. 15, no. 8, p. 909-911.
- Turcotte, D. L., 1992. Fractals and chaos in geology and geophysics. Cambridge University Press, Cambridge.
- Walsh, J. J., and Wattersen, J., 1993, Fractal analysis of fracture patterns using the standard box-counting technique: valid and invalid methodologies; Brevia, in *Journal of Structural Geology*, vol. 15, no. 12, pp. 1509-1512.
- Wilson, T. H., 1987, Structural Analysis of the Parsons CSD across the Middle Mountain Syncline and Elkhorn Mountain Anticline: *Northeastern Geology*, vol. 9, no. 3, pp 161-184.
- Wilson, T. H., and Dominic, J., in review, Fractal interrelationships between topography and structure: by the *British Journal of Geomorphology Earth Surface Processes and Landforms*.

M97002294



Report Number (14) DOE/MC/32158--5662

Publ. Date (11) 19960903

Sponsor Code (18) DOE/FE, XF

JC Category (19) UC-101, DOE/ER

DOE